surfaces

MDPI

Article

Development of a Colorimetric Polydiacetylene, Solid-Substrate Sensor for SARS-CoV-2 Detection in Human Saliva

Christopher T. Stueber [1,2,3], Timothy W. Hanks [1,*], Paul L. Dawson [4,*], Julie K. Northcutt [4], William T. Pennington [5] and Belinda Cochran [4]

1 Department of Chemistry, Furman University, Greenville, SC 29613, USA; chris.stueber@outlook.com
2 Center for Immunology and Inflammatory Diseases, Department of Medicine, Massachusetts General Hospital, Boston, MA 02114, USA
3 Krantz Family Center for Cancer Research, Mass General Cancer Center, Boston, MA 02114, USA
4 Department of Food, Nutrition and Packaging Sciences, Clemson University, Clemson, SC 29634, USA; jknorth@clemson.edu (J.K.N.); bcohra@clemson.edu (B.C.)
5 Department of Chemistry, Clemson University, Clemson, SC 29634, USA; billp@clemson.edu
* Correspondence: tim.hanks@furman.edu (T.W.H.); pdawson@clemson.edu (P.L.D.)

Abstract

The SARS-CoV-2 pandemic caused tremendous loss of life and long-term health effects for many. The virus continues to evolve, and new variants have the potential to cause widespread physical and economic impacts. Long-chain carboxylic acids featuring two conjugated acetylenes midway along the chain easily self-assemble onto various substrates, particularly polyvinylidene fluoride, and then polymerize to form a deep blue film. COVID-19 nucleocapsid or spike protein antibodies can be conjugated to the film, and upon exposure to appropriate trigger proteins, they turn pink or red. Certain additives commonly found in commercial preparations of COVID-19 proteins can trigger false positives. The addition of small amounts of surfactants can increase detector sensitivity, though this must be carefully controlled to avoid false positives. Sensing systems based on both nucleocapsid and ACE2 antibodies can detect authentic samples of the virus in human saliva. The platform is readily adaptable to antibodies from new variants.

Keywords: COVID-19; biosensor; polydiacetylene; antibody; saliva

check for updates

Academic Editor: Mark Biggs

Received: 21 September 2025
Revised: 3 November 2025
Accepted: 8 November 2025
Published: 11 November 2025

Citation: Stueber, C.T.; Hanks, T.W.; Dawson, P.L.; Northcutt, J.K.; Pennington, W.T.; Cochran, B. Development of a Colorimetric Polydiacetylene, Solid-Substrate Sensor for SARS-CoV-2 Detection in Human Saliva. *Surfaces* **2025**, *8*, 79. https://doi.org/10.3390/surfaces8040079

Copyright: © 2025 by the authors. Licensee MDPI, Basel, Switzerland. This article is an open access article distributed under the terms and conditions of the Creative Commons Attribution (CC BY) license (https://creativecommons.org/licenses/by/4.0/).

1. Introduction

Severe acute respiratory syndrome coronavirus 2 (SARS-CoV-2) was responsible for the COVID-19 pandemic and has had profound global impacts on public health, national economies, and daily life. It caused millions of deaths and strained healthcare systems worldwide. The pandemic led to widespread lockdowns, travel restrictions, and economic disruptions, resulting in job losses and financial instability. SARS-CoV-2 is the third coronavirus since 2000 to display cross-species infection, causing respiratory disease, including one in 2003 and another in 2012 [1]. SARS, as well as other viral and bacterial agents, continues to threaten global pandemics, and their rapid detection would mitigate the spread and impact of these pathogens. Currently, the SARS-CoV-2 diagnostic tests approved by the Food and Drug Administration fall into two categories: (1) RNA detection-based (molecular tests), also known as reverse transcription polymerase chain reaction (RT-PCR) testing that detects genetic material, and (2) serological immunoassay (antibody/antigen)-based tests that detect viral proteins [2–4]. In RT-PCR, SARS-CoV-2 RNA is reverse transcribed to DNA and amplified to obtain a signal, which, in turn, identifies the presence of the virus

with 95% accuracy and can quantify the number of viral particles by the number of rounds of amplification required to obtain a signal [5,6]. However, molecular tests suffer from limitations of speed and volume (number of samples) and require specialized, expensive equipment that must be operated by highly trained individuals. For example, surface plasmon resonance and electrochemical detection methods are extraordinarily sensitive but are not suitable for initial screening under field conditions. Serological antibody tests measure past exposure, frequently detect other non-SARS-CoV-2 antibodies, and are often misinterpreted because a negative test does not necessarily mean a lack of exposure.

Serological tests detect specific proteins unique to the viral particle surface, such as the spike protein, which distinguishes SARS-CoV-2 as a coronavirus and functions to recognize host cell receptors [7]. Since each viral particle has, on average, 100 spike protein copies on its surface, the spike protein is a good target for serological tests to detect the virus [8]. The spike protein promotes binding of SARS-CoV-2 to the human angiotensin-converting enzyme 2 (ACE2) to initiate the process of viral replication. Thus, ACE2 can function to target the SARS-CoV-2 virus [9]. Another potential viral protein that can be used for serological tests is the nucleocapsid protein (N-protein). The N-protein is an abundant and highly conserved protein in the SARS-CoV-2 virion that promotes lung inflammation and suppresses the immune response [10,11].

Apart from RT-PCR testing, enzyme-linked immunosorbent assays (ELISAs) are used to detect antibodies in blood or nasal samples, where labeled secondary antibodies are used to detect and quantify SARS-CoV-2 viral infection [12]. There are various types of ELISA techniques; however, they all have an antibody bound to a substrate that captures the target antigen. A detection antibody is then added that effectively sandwiches the target antigen, yielding a color response from a substrate that will link to the antibody [13]. The immune system produces IgG, IgM, and IgA within 7 days of infection, and infected subjects have detectable levels of antibodies by 15 days post-infection [14,15]. Roy et al. [12], among others, developed ELISA-based SARS-CoV-2 assays using antibodies that target the receptor-binding domain since it is a relatively stable structure compared to other viral components. ELISAs provide information on both active and past infections and can analyze thousands of samples in labs with resource-limited settings. Thus, ELISAs can be used in disease surveillance programs to assess the rate of infection among the community [16].

Because of the difficulties and restrictions with current viral diagnostic tests, new efficient methods for rapid and reliable detection of SARS-CoV-2 are still needed. Biosensors, especially those that provide rapid and sensitive single-step detection, are viewed as acceptable alternatives to RT-PCR and serological tests. Another method for biological molecule recognition is the use of derivatized polydiacetylenes. Polydiacetylenes (pDAs) are formed by the photoreaction of self-assembled diacetylenes (DAs), which were first synthesized in the 1960s [17] and first investigated in the 1990s by Charych et al. as an influenza sensor [18]. When exposed to external stimuli (including surface molecular binding), a rotation about the C—C bonds of the pDA backbone shifts the optical appearance of the polymer from blue to red [12]. Much of the work in this area has focused on pDAs in the form of solution-dispersed vesicles or liposomes. However, such structures in aqueous solutions have several limitations, including the high analyte concentration needed to obtain a sensor response, sensitivity to other unrelated stimuli, and production scale-up [19]. To address pDA solution-based sensor limitations, substrate-mounted pDAs have been developed [20], including several reports that have successfully utilized polyvinylidene fluoride (PVDF) membranes as pDA-supporting substrates [21–24].

Several pDA sensors have been developed for bacteria using aptamers [25], phospholipids [26], and amino acids [27]. The ability to conjugate probes to pDA on substrates

that target specific receptors, such as antibodies unique to viral particles, allows for the development of a variety of viral sensors. Conjugation of antibodies (Ab) to pDA materials is typically achieved through the chemical reaction of an N-hydroxysuccinimide (NHS)-derivatized pDA and an amine group (-NH_2) on the Ab [28]. For example, Son et al. [29] and Jeong et al. [21] used NHS-derivatized pDA and a phospholipid, 1,2-dimyristoyl-sn-glycero-3-phospho-choline (DMPC), immobilized onto PVDF, before functionalizing with influenza A-specific antibodies. These researchers reported successfully detecting the virus with an optical blue-to-red color change on antibody-conjugated PVDF-pDA viral sensors. The adaptation of pDA sensors to detect SARS-CoV-2 was reported by Prainito [30] and by Li [31].

Here, 10,12-pentacosadiynoic acid (PCDA) is deposited on various substrates in order to determine the most suitable for testing. The films were then photopolymerized to deep blue pDA and exposed to potential environmental stimuli that might trigger false positives. Next, films made from mixtures of PCDA and its NHS ester were deposited and polymerized. These were then conjugated to COVID-19 antibodies and exposed to the corresponding antigens. It was found that sensitivity could be improved by the addition of controlled amounts of surfactants. Ultimately, the sensors were found to be able to detect the COVID-19 virus in human saliva. A key innovation of this sensor is its ease of use by untrained individuals and adaptation for the rapid testing of large numbers of samples without specialized equipment. Furthermore, viral protein/antibody groups can be used to create multiple sensors that can be co-located on a single matrix to minimize false negative results. Our proposed polydiacetylene (pDA) sensors bridge the gap between molecular tests and serological antibody tests by detecting active infections (virus proteins) and past exposure (antibodies) in a single platform.

2. Materials and Methods

2.1. General

2.1.1. Materials

10,12-pentacosadiynoic acid (PCDA) was acquired from GFS Chemicals (Columbus, OH, USA), purified immediately prior to use by dissolving in dichloromethane, and filtering through a 0.2 μm syringe filter. After purification, the material was a solid that was only manipulated in the dark. N-hydroxysuccinimide (NHS), 1-ethyl-3-dimethylaminopropylcarbodiimide hydrochloride (EDC), and NP-40 Surfact-Amps™ (nonyl phenoxypolyethoxylethanol) detergent were purchased from Thermo Fisher Scientific (Waltham, MA, USA). Triton X-100 was purchased from Sigma Aldrich (Burlington, MA, USA). Recombinant human novel coronavirus nucleoprotein (N), N-Antibody, recombinant human novel coronavirus spike glycoprotein (S), S-antibody, and recombinant human angiotensin-converting enzyme 2 (ACE2) were purchased from Cusabio (Houston, TX, USA). SARS-CoV-2 (COVID-19) spike ELISA pairs were purchased from GeneTex (Irvine, CA, USA) and used as received. COVID-19-positive saliva (Delta and Omicron) samples were provided by the COVID-19 Testing Laboratory at Clemson University, Clemson, SC, USA. All COVID-19 positive samples used were confirmed by RT-PCR prior to testing. All other compounds, reagents, and solvents used were purchased from commercial houses and used as received, unless otherwise indicated. Distilled water was obtained from a PURELAB Chorus 1 Complete purification system from Elga Water (High Wycombe, UK). Immobilon-PSQ PVDF membranes were purchased from Millipore Sigma (St. Louis, MO, USA). Polypropylene and nylon membranes were purchased from Tisch Scientific (Cleves, OH, USA). Nylon, acrylic, polyester, and cotton fabrics were purchased from TestFabrics Inc. (West Pittston, PA, USA).

2.1.2. Instrumentation

NMR data were collected on a JEOL JNM-ECZL spectrometer (Peabody, MA, USA) with a proton frequency of 500 MHz. Infrared spectra were acquired with a Perkin Elmer Spectrum 100 FT-IR (Shelton, CT, USA) using an attenuated total reflectance accessory, while electronic spectra were acquired on a Cary 60 UV-Vis (Agilent, Santa Clara, CA, USA). Diacetylene polymerization was affected by exposure to a Mineralight UVG-11 Lamp (Analytik Jena US, Upland, CA, USA) at 254 nm.

2.1.3. Purification and Filtration Supplies and Substrate Storage

Solutions of PCDA were filtered through 7K MWCO regenerated cellulose syringe filters that were purchased from Thermo Fisher (Waltham, MA, USA). An electronic humidity control storage unit was used to store substrate sensors. A Thermo Fisher Scientific (Waltham, MA, USA) accuSpin Micro 17R centrifuge was used to concentrate COVID-19-positive saliva samples, and a Corning LSE Digital Dry Bath (Thermo Fisher, Waltham, MA, USA) was used to denature live viral particles, prior to testing when necessary. All pDA-based sensors treated with COVID-19-positive saliva samples were tested in a LABCONCO Logic^{+} (Kansas City, MO, USA) sterile laboratory hood.

2.2. Synthesis of Precursors

2.2.1. Synthesis of PCDA-NHS Monomer

An NHS ester was prepared as previously described [21]. Briefly, PCDA (0.500 g, 1.33 mmol) was dissolved in 25 mL of dichloromethane (DCM) and filtered through a 0.2 μm cellulose acetate syringe filter to remove any of the bright blue polymer that forms upon storage, even in the dark. The solvent was removed in vacuo. The flask was purged with dry N_2. Dry, deoxygenated DCM (25 mL) was added, and the solution was stirred for 20 min to ensure complete dissolution of the PCDA. NHS (0.174 g, 1.51 mmol) and EDC (0.294 g, 1.89 mmol) were added, and the mixture was stirred for 4 h. at room temperature. The product mixture was washed 3 times with distilled water. The organic layer was dried with $MgSO_4$, then filtered, and the solvent was removed. The white powder was stored at 4 °C under N_2. The ^{1}H NMR (500 MHz, DMSO-d^6, ppm) was as follows: δ 2.80 (m, 4H, 21), 2.65 (t, 2H, 1), 2.27 (t, 4H, 8,9), 1.61 (t, 2H, 2), 1.43 (br, 4H, 7,10), 1.32–1.24 (br, 26H, 3–6,11–19), 0.85 (t, 3H, 20). The IR data were consistent with previous reports [30].

2.2.2. Preparation of Stock Solutions

Appropriate amounts of purified PCDA or PCDA-NHS were dissolved in DCM to make 2.5 mM and 0.10 mM solutions, respectively. These solutions were purged with argon and stored at 4 °C.

2.2.3. Ethanolamine/PBS Stock Solution

Ethanolamine (EtAm, 120 μL, 16.6 M) and a phosphate-buffered solution (PBS, 1.0 L) were added to a volumetric flask. The resulting 2 mM EtAm/PBS solution was transferred to an amber bottle and stored until later use.

2.3. Sensor Production and Testing

2.3.1. General Overview

Substrates were briefly soaked in a mixture of PCDA and PCDA-NHS and then dried and photopolymerized to a blue polymer. The sensor substrates were exposed to various aqueous solutions designed to test the effects of pH, the presence of surfactants, and the effect of additives commonly found in commercial antibody and protein samples. The desired antibodies were conjugated to the PCDA through a substitution reaction of PCDA-

NHS in PBS buffer. In some cases, EtAm was used to deactivate unreacted PCDA-NHS. The sensor chips were then exposed to PBS solutions containing virus proteins or denatured or active virus samples.

2.3.2. Production of pDA/pDA-NHS Substrate Platforms

Swatches of a substrate material, including nylon, polyester, cellulose, acrylic, cotton, polyvinylidene fluoride, polypropylene, graphene paper, and cellulose filter paper, were cut to size (2.5 cm × 2.5 cm) and placed in glass petri dishes on top of filter paper. PCDA (5 mL, 2.5 mM) and PCDA-NHS (5 mL, 0.1 mM) from stock solutions were added to each dish. These were then covered with parafilm, placed on a plate shaker, and gently agitated for 1 min. The substrates were then removed from the monomer solution dish and placed on a fresh piece of filter paper to absorb excess fluid. The dish was then stored in a dark, dry environment and allowed to dry for 12 h. The substrates were then placed under a UV lamp (254 nm) for 60 s. To ensure uniform polymerizations, they were rotated 90° every 15 s. The blue pDA substrates were then stored in a dark, dry environment until COVID-19 probe conjugation.

2.3.3. PCDA Sensor Synthesis

A single uniformed polymerized pDA/pDA-NHS substrate square was added to a clean, sterile vial. A sterile pipette was used to add autoclaved PBS (2.5 mL) to the vial. A micropipette was then used to add approximately 25 µg of the chosen COVID-19 antibody probe (ACE2, spike antibody, nucleoprotein antibody, ELISA Kit spike antibody) to the vial with the PVDF-pDA membrane. The vial was then placed on the plate shaker, and the conjugation reaction was allowed to run for 3 h at 4 °C. In some cases, any remaining NHS groups were deactivated by removing the COVID-19 probe solution, followed by the addition of EtAm/PBS solution (2 mM) or BSA (150 µg/mL) in HEPES buffer (2.5 mM). The vial was placed back on the plate shaker, and the deactivation reaction was allowed to run for 1 h at 4 °C. The sensors were then removed from the vials and washed with sterile water. Once washed, the PVDF-pDA-SARS-CoV-2 substrate sensors were sealed in new sterile petri dishes, dried, and stored in a dark, dry environment until testing. Successful conjugation of the chosen COVID-19 probe was confirmed by IR spectroscopy.

2.3.4. Sensor Testing Protocol

Typically, a PVDF-pDA sensor conjugated to an antibody was treated with a 20 µL drop containing a corresponding trigger protein at a concentration of 1.0 to 4.0 µg. In some cases, due to the high hydrophobicity of the PVDF material, the trigger solution contained trace amounts of surfactant. Alternatively, the substrate was dipped in a buffer solution containing the surfactant, prior to testing with the trigger solution, to speed up the reaction as well as increase the surface area of the reaction between the membrane surface and the trigger solution.

3. Results

3.1. Sensor Preparation

3.1.1. Selection of a Sensor Substrate

pDAs in the form of self-assembled monolayers, multilayers, and liposomes have been used in sensing applications. For ease of manipulation and long shelf-life, the assembly of PCDA onto a smooth, inexpensive, thin, and flexible substrate is ideal. Numerous substrates have been investigated as supports for pDA sensors, including glass [32,33], silica [34], agarose [35], alginate fiber [36], graphene sheets [37], sol–gel matrices [38], cellulose [39], polyvinylidene fluoride (PVDF) membranes [21,24,40], and others [41]. In

order to conjugate a probe to the pDA, the hydrophilic end of the NHS-derivatized PCDA must be exposed. As the substrate coating process could result in either monolayers or multilayers, it was not clear what sort of surface would be best. It is well understood, however, that PCDA coatings must be highly organized in order to undergo the topotactic photopolymerization required to form blue pDA.

Figure 1 shows the results of soaking various potential substrates in a DCM solution of PCDA, followed by drying and exposure to UV radiation. The substrates evaluated included fabric surfaces, such as nylon, polyester, acrylic, and cotton, as well as membrane surfaces, such as PVDF, polypropylene, graphene (hydrophobic paper), and cellulose filter paper.

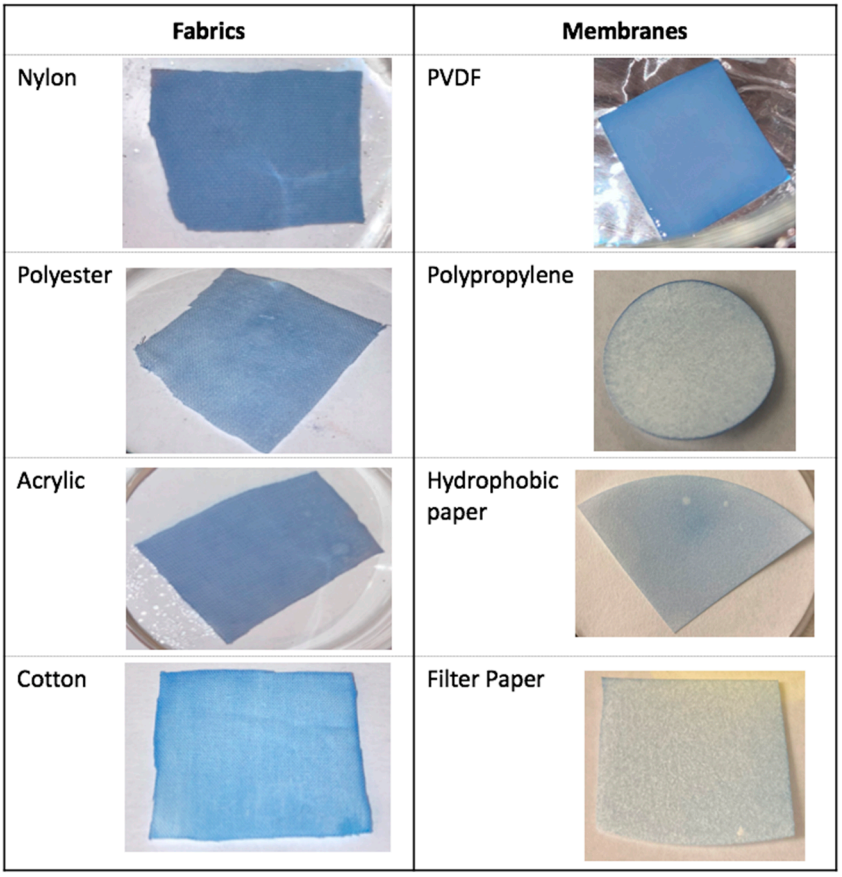


Figure 1. Photographs of various substrate materials soaked in a DCM solution of PCDA for 60 s, dried, and photolyzed by UV light for 60 s with a 90° rotation every 15 s.

Polypropylene, graphene (hydrophobic)- and cellulose (filter)-based papers, and cotton were rejected as suitable substrates due to poor coating performance. Polyester and acrylic were deemed to be marginal, while nylon and especially PVDF appeared most promising. Nylon offered a rougher surface, with a greater surface area, while the PVDF surface was very uniform and stiffer, making manipulation of the substrate easier, both in terms of conjugating probe molecules and reducing the potential for contamination. These were considered for further development.

3.1.2. General Synthesis Procedure

The most common method for derivatizing PCDA for sensing applications is the conversion of the compound into its NHS ester derivative after an initial reaction with EDC. The NHS group is easily displaced by a nucleophilic primary amine, such as those found in many proteins and antibodies. While the probes could be attached to the PCDA at

the monomer stage, this was avoided as large headgroups could disrupt the organization of the DAs when deposited on the substrate. The UV irradiation required to trigger the polymerization had the potential to degrade the probe antibody in such cases. Instead, a mixture of PCDA and PCDA-NHS in a 95:5 ratio was deposited, followed by irradiation. The probe conjugation was then performed on the PVDF-pDA surface. The process was monitored by FT-IR (Figure 2). Introduction of PCDA showed a carbonyl stretch around 1700 cm^{-1} for the PCDA carboxylic acid. The ACE2 product shows the amide I and II bands at ~1600 and 1490 cm^{-1}, respectively.

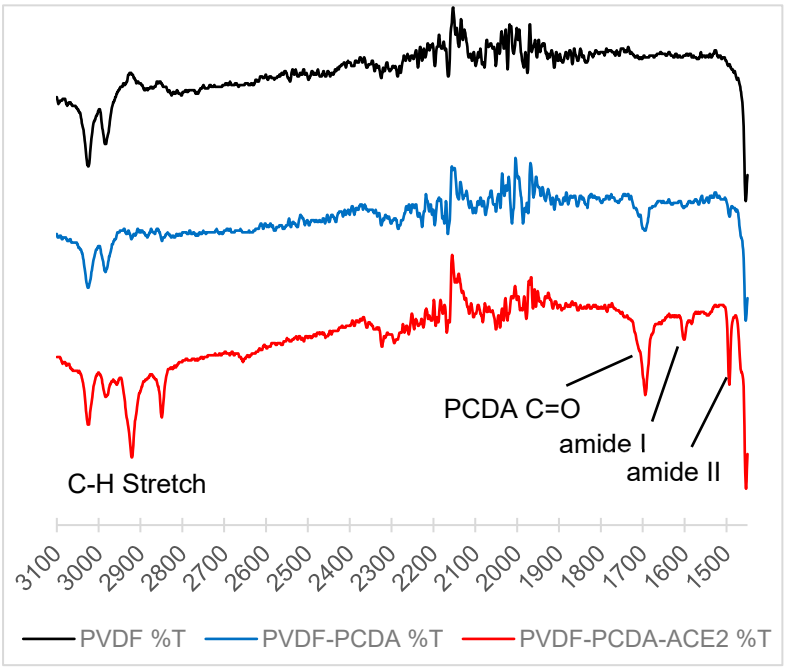


Figure 2. Stacked IR of PVDF (black line), PVDF-PCDA (blue line), and PVDF-PCDA-ACE2 (red line) (top). The amide I and amide II bands of ACE2 can clearly be seen at 1600 and 1490 cm^{-1}, respectively.

3.2. pH and Surfactant Effects on the Sensor Platform

The candidate substrates, particularly PVDF, were very hydrophobic, resulting in a poor interaction between aqueous proteins and the sensing probes. Figure 3a shows how a drop of DI water beads up on a pDA/PVDF surface. A 10% solution of Triton-X (Figure 3b) reduced the contact angle but triggered a sensor color change. However, reducing the Triton-X concentration to 0.01% still allowed for sufficient wetting of the substrate without causing the color change (Figure 3c). Thus, the addition of surfactants in small amounts was found to be important for the best sensor performance. Figure 4 shows the performance of a PVDF-pDA substrate coupled to the antibody of the SARS-CoV-2 nucleocapsid protein (N-protein). The nucleocapsid protein is the most conserved and abundant component of the SARS-CoV-2 viral particle, though it is not expressed on the virus surface. Here, the sensor was dipped in a dilute aqueous solution 0.01% of TritonX. This was then rinsed with DI water before being exposed to a drop of a solution containing 10 µL of the N-protein in PBS. This resulted in the triggering of the sensor. Without the surfactant, the solution only poorly wetted the sensor surface, and the color change was minimal (Figure 4c). The addition of the surfactant to the N-protein solution also allowed for good wetting of the surface and an excellent color change (Figure 4d). The color change was apparent after 1 min, with the color shift becoming greater after 90 s.



(**a**) (**b**) (**c**)

Figure 3. Three pDA/PVDF sensors exposed to (**a**) DI water, (**b**) 10% Triton-X solution, and (**c**) 0.01% Triton-X solution.



(**a**) (**b**) (**c**) (**d**)

Figure 4. Isolated SARS-CoV-2 nucleocapsid protein detection using the PVDF-pDA-N-Antibody substrate sensing platform. (**a**) Dipped in 0.01% Triton in PBS only, (**b**) dipped in 0.01% Triton in PBS and then 10 µL of a 0.57 mg/mL solution of N-protein in PBS, (**c**) 10 µL of a 0.57 mg/mL solution of N-protein in PBS only, and (**d**) 20 µL of a solution containing Triton 0.01% Triton and 0.57 mg/mL N-protein.

The color change of pDA sensors can be triggered by various stimuli, which could result in false positives if not understood. High pH or temperature are the most obvious concerns; however, some surfactants and sanitizers also trigger the sensors [42], and other additives to either antibodies or proteins potentially could do the same. Figure 5 provides a visual representation of the effect pH sensitivity has on the pDA coatings on PVDF. Below a pH of 10, the blue form of pDA was indefinitely stable. At a pH of 11, a slight color change to pink was observed after 24 h, but at pH 13, the color change was immediate. In all subsequent experiments, the pH was maintained below 10.

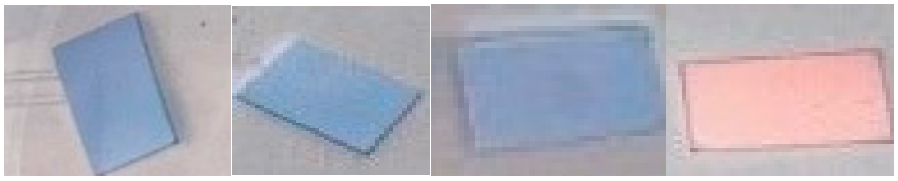


Figure 5. Four pDA/PVDF sensors at pH (from **left** to **right**) 9, 10, 11, and 13.

The ability to maintain a pH of 10 or lower during testing conditions became apparent as commercial sources of spike and nucleocapsid proteins (N protein) were delivered in phosphate buffers, some of which were found to have relatively high pH. Probes were prepared by coupling the ACE2 antibody to pDA on a nylon substrate, followed by exposure to the spike protein (Figure 6). The protein was obtained from two sources, which behave differently. Both showed a modest color change between the controls (Figure 4a,c) and the ACE2 antibody-modified surfaces (Figure 4b,d); however, the protein in the slightly more basic buffer triggered color changes on its own. In the control experiments, we found that the addition of reconstituted probes with lyophilized PBS additives or solution-based probes with PBS and other phosphate additives did not trigger a color response. Thus, the color change seen during testing may have been enhanced by the specifics of the phosphate buffer in addition to the conjugate probe-to-trigger interactions. The nylon sensors seemed to be more pH-sensitive than the PVDF sensors; thus, the latter became the surface of choice based on performance in preparing the sensor and detecting the sensor response. Others have also found this to be the preferred substrate for sensing applications [43].



(**a**) (**b**) (**c**) (**d**)

Figure 6. Four pDA-ACE2-antibody nylon membranes exposed to different PBS buffers at different pH values with and without spike protein exposure for 10 min at (**a**) pH 7.2 without ACE2 spike protein, (**b**) pH 7.2 with ACE2 spike protein at 0.1 mg/mL, (**c**) pH 8.0 without ACE2 spike protein, and (**d**) pH 8.0 with ACE2 spike protein at 0.1 mg/mL.

3.3. Effects of Other Additives

In addition to the differences observed as a result of pH, other potential interferences could arise from buffers, salt, and sugar mixtures that are used as "carriers" in commercial protein/antibody SARS preparations. Thus, a series of tests was conducted to determine which, if any, of these additives caused a sensor response that could lead to false positives during testing. As discussed previously, the surfactant was important in triggering the color change more rapidly, and upon further evaluation, NP-40 was found to be superior to Triton-X in this role due to the lower overall pH of NP-40 as compared to Triton-X (5.1 vs. 6.2, respectively). Furthermore, NP-40 is a preferred surfactant for use to solubilize lipids and proteins. The additives tested with and without the NP-40 surfactant are shown in Tables 1 and 2, respectively, and include 20 mM Tris-HCl (20 µL, 0.5 M NaCl (20 µL), 6% Trehalose (20 µL), 20 mM Tris-HCl + 0.5 M NaCl + 6% Trehalose (1:1:1 ratio), 20 mM Tris-HCl + 0.5 M NaCl (1:1 ratio), 20 mM Tris-HCl + 6% Trehalose (1:1 ratio), and 0.5 M NaCl + 6% Trehalose (1:1 ratio).

Table 1. Color response (0–4) of PVDF-PDCA membranes to various additives without NP-40 added.

Chemical	0 min	5 min	15 min	30 min	60 min	75 min	120 min	180 min	24 h
20 mM Tris-HCl	0 [1]	0	0	0	0	0	1	1.5	2
0.5 M NaCl	0	0	0	0	0	0	0	0	0
6% Trehalose	0	0	0	0	0	0	1	1	1
20 mM Tris-HCl + 0.5 M NaCl + 6% Trehalose	0	0	0	0	0	0	0	0	1
20 mM Tris-HCl + 0.5 M NaCl	0	0	0	0	0	0	0	0	2.5
20 mM Tris-HCl + 6% Trehalose	0	0	0	0	0	0	0	1	1
0.5 M NaCl + 6% Trehalose	0	0	0	0	0	0	0	0	0

[1] 0 = no color to 4 = bright pink color.

It was observed that trehalose was the least hydrophobic of the additives tested, spreading on the membrane after 45 min. Tris-HCl (with and without NP-40) gave the greatest intensity of pink color development when applied individually (Tables 1 and 2), and, with the surfactant NP-40 added, all combinations using Tris-HCl turned the membrane pink. However, without a surfactant, all combinations using Tris-HCl also turned pink, just to a lesser degree than that achieved when paired with NP-40. The positive response to Tris-*HCl* may be due to its weak acid property, resulting in the donation of a proton, or its interaction with the nitrogen/carboxyl groups on the sensor. These results allowed us to identify potential false positives when using commercial SARS protein/antibody samples; however, this would not be an issue in the testing of human saliva samples, or at least negative controls could be included on the sensor platform to minimize false positive results.

Table 2. Color response (0–4) of PVDF-PDCA membranes to various additives with NP-40 added.

Chemical	0 min	5 min	15 min	30 min	60 min	75 min	120 min	180 min	24 h
20 mM Tris-HCl	1 [1]	1	1.5	2	3.5	4	4	4	4
0.5 M NaCl	0	0	1	1	1	1	1	1	1
6% Trehalose	0	0	1	1	1	1	1	1	1
20 mM Tris-HCl + 0.5 M NaCl + 6% Trehalose	1	1	2	3	3	3	3	3	3
20 mM Tris-HCl + 0.5 M NaCl	1	1	3	4	4	4	4	4	4
20 mM Tris-HCl + 6% Trehalose	0	0	1	1	4	4	4	4	4
0.5 M NaCl + 6% Trehalose	0	0	0	1	1	1	1	1	1

[1] 0 = no color to 4 = bright pink color.

3.4. Sensor Performance Against Model Antibodies

3.4.1. N-Antibody vs. N-Protein

The N-protein has been reported to recognize four protein and three sugar receptor sites of the coronavirus protein, which may make this probe more sensitive than the spike protein. In addition, the N-protein has a "linker" region that has been found to interact with the membrane protein [44,45]. As such, the PVDF-pDA sensors were conjugated with nucleocapsid protein under standard conditions, and the remaining unreacted pDA-NHS sites were deactivated by treatment with EtAm. Table 3 shows the results of treating the substrate surfaces with trigger solutions. The control sensors without a conjugated antibody showed no significant response to PBS buffer, regardless of whether a surfactant was added or if the sensor was heated. Likewise, the antibody-conjugated sensors did not respond to solutions without a trigger protein. Finally, the conjugated sensors exposed to solutions containing the trigger protein did show some response, but this was greatly enhanced by the presence of the surfactant and even more so by heating at 40 °C for a short period.

Table 3. Response to combinations of a nucleoprotein antibody probe on the sensors with levels of SARS-CoV-2 nucleoprotein trigger and NP-40 surfactant, with deactivation of unbound NHS sites and heating at 40 °C.

N-Pro Ab Probe	N-Pro Trigger (µg)	NP-40	Time at 40 °C	Response
25 µL (25 µg)	5.0	0.02% 10 µL		+ bright 
25 µL (25 µg)	5.0	none		-
25 µL (25 µg)	0	0.02% 10 µL		-
25 µL (25 µg)	0	0.02% 10 µL	60 s	-
25 µL (25 µg)	5.0	0.02% 10 µL	60 s	+ bright
none	5.0	0.02% 10 µL		dull color
none	5.0	none		-
none	0	0.02% 10 µL		-
none	0	0.02% 10 µL	60 s	-
none	5.0	0.02% 10 µL	60 s	dull color

Similar results were observed even if the residual NHS esters were not deactivated with EtAm. Once again, only the treatments with the probe, trigger, and surfactant responded

definitively with a blue-to-red transition within 60 s (Table 4). Thus, the deactivation step was found to be unnecessary.

Table 4. Response to combinations of a nucleocapsid protein antibody probe on sensors with levels of SARS-CoV-2 nucleocapsid protein trigger and nonyl phenoxypolyethoxylethanol surfactant (NP-40) and heating at 40 °C.

N-Pro Ab Probe	N-Pro Trigger (µg)	NP-40	Time at 40 °C	Response
25 µL (25 µg)	5.0	0.02% 10 µL		+ bright 
25 µL (25 µg)	5.0	none		-
25 µL (25 µg)	0	0.02% 10 µL		-
25 µL (25 µg)	0	0.02% 10 µL	60 s	-
25 µL (25 µg)	5.0	0.02% 10 µL	60 s	+ bright 
none	5.0	0.02% 10 µL		dull color
none	5.0	none		-
none	0	0.02% 10 µL		-
none	0	0.02% 10 µL	60 s	-
none	5.0	0.02% 10 µL	60 s	dull color

Since the addition of the surfactant NP-40 was needed to facilitate the sensor color response, briefly soaking the PVDF sensor in a 0.02% NP-40 solution in PBS during sensor production was tested to determine if the addition of a surfactant to the trigger solution during testing could be avoided. This process was successful, with a blue-to-red color change only in the test strips that had been previously dipped in NP-40. However, following testing, there were slight color changes in the test strips after drying that did not have both the probe and trigger present [false positives] (Table 5). Thus, a surfactant could be added during the sensor manufacturing process rather than during the testing phase.

Table 5. Response to combinations of a nucleoprotein antibody probe on sensors with levels of SARS-CoV-2 nucleoprotein trigger dipped in NP-40 surfactant during production, with deactivation of unbound NHS sites and heating at 40 °C.

N-Pro Ab Probe	N-Pro Trigger (µg)	NP-40	Time at 40 °C	Response
25 µL (25 µg)	5.0	0.02%		+ bright 
25 µL (25 µg)	5.0	none		- pink when dry
25 µL (25 µg)	0	0.02%		-
25 µL (25 µg)	5.0	0.02%	60 s	+ bright 
none	5.0	0.02%		dull color
none	5.0	none		- pink when dry
none	0	0.02%		-
none	5.0	0.02%	60 s	dull color 

3.4.2. ACE2 Antibody vs. Spike Protein

To further optimize the sensor response, matching ELISA pairs of spike protein/spike antibody were used for the pDA probe with the matching antibody as the trigger. The pDA sensors were created using Capture Antibody SARS-CoV-2 (COVID-19) spike antibody [1A9] (GTX632604), and these were exposed to Detection Antibody SARS-CoV-2 (COVID-19) spike S1 antibody [HL13402] (GTX635713). The objective of these tests was to use SARS-CoV-2 (COVID-19) spike ELISA pairs [1A9/HL13402] to evaluate the selectivity and reactivity of the sensors when exposed to a surfactant along with the trigger.

We previously determined that the surfactants interact with the pDA sensors to enhance trigger color change. Therefore, varying concentrations of probes were tested with different amounts of surfactants (Table 6). The spike receptor-binding protein (RBP) trigger was diluted to a concentration of 0.2 μg/μL; then 5, 10, 15, or 20 μLs of the diluted spike (RBP) trigger was dispensed atop the pDA sensor surface, resulting in additions of 1.0, 2.0, 3.0, and 4.0 μg of spike RBD (receptor-binding protein) to the sensor, respectively. The surfactant at 0.1% gave a positive response at the 1 to 4 μg concentrations of the SARS RBD trigger. When 0.01% NP-40 was added, only the 4.0 μg concentration of NP-40 gave a positive response. Treatment of the pDA-PVDF sensors with the ELISA nucleocapsid protein did not trigger a response even with a surfactant and heating, thus indicating the specificity of these sensing platforms utilizing matching ELISA pairs.

Table 6. Response to combinations of anti-SARS-CoV-2 spike protein antibody probe on sensors with different levels of SARS-CoV-2 spike receptor-binding protein (RBD) trigger and the NP-40 surfactant.

Spike Ab Probe (μg)	SARS RBD Trigger (μg)	%NP-40	Response
20	1.0	0.01	-
20	2.0	0.01	-
20	3.0	0.01	~
20	4.0	0.01	+
20	1.0	0.1	+
20	2.0	0.1	+
20	3.0	0.1	+
20	4.0	0.1	+

3.5. Testing Biosensor Membranes Against Denatured and Active Viruses

3.5.1. General

Active human SARS-CoV-2 saliva samples were obtained from the Clemson University COVID-19 Development Laboratory. This laboratory retained COVID-19 samples, including positive samples, from the testing facility on Clemson's campus. All faculty, staff, and students were tested regularly, and positive samples were stored for determining variants and use in additional research. Test samples were typically heat-inactivated at 90 °C for 30 min for testing in the campus-monitoring program. In addition, saliva COVID-19-positive samples that had not been denatured were retained and tested by trained personnel under strict safety protocol.

3.5.2. Testing Summary

The PVDF-pDA-spike-antibody and PVDF-pDA-N-Antibody membrane sensors were tested against positive COVID-19 saliva samples (Delta and Omicron variants)—some heat-inactivated at 90 °C for 30 min and others still active. A total of 12 pDA spike antibody and 12 N-protein antibody membranes were tested against active Omicron and active Delta SARS-CoV-2 variants. Control samples of saliva from negative COVID-19 samples were also tested, showing no color change even after 4 days. The PVDF-pDA-spike-antibody

membranes showed little to no immediate response to the virus, and the color change from blue to red (pink) was not immediately observed. It was determined that our spike antibody did not have specificity towards the Omicron spike proteins, explaining the lack of color change. We were able to test the PVDF-pDA-spike-antibody sensors against a possible COVID-19 Delta saliva sample, and after some time, a faint color change was possibly observed (though not in real time as hoped), as well as a distinct red circle on the membrane. Additionally, the PVDF-pDA-spike-antibody sensors were tested against denatured, inactive COVID-19 virus (Omicron) saliva samples, and, again, no immediate color change was observed in real time. These results were expected as the spike protein on the surface of the virus cannot be targeted once denaturing breaks open the viral particle.

Due to the variations in spike proteins among the different COVID-19 variants, it was determined that the best route for targeting live COVID-19 virus may be through ACE2, as the specificity between ACE2 and the spike protein remains fairly constant from variant to variant (Figure 7). Since the ACE2 used was synthesized originally for the Delta variant spike protein, the bottom-row sensors, tested against the Delta variant, yielded more distinctive results than the top-row sensors, tested against the Omicron variant. However, the ACE2 we used still should have had some level of recognition towards the Omicron variant spike protein, and, indeed, though lesser in intensity, a color change was observed in sensors tested against Omicron saliva samples.

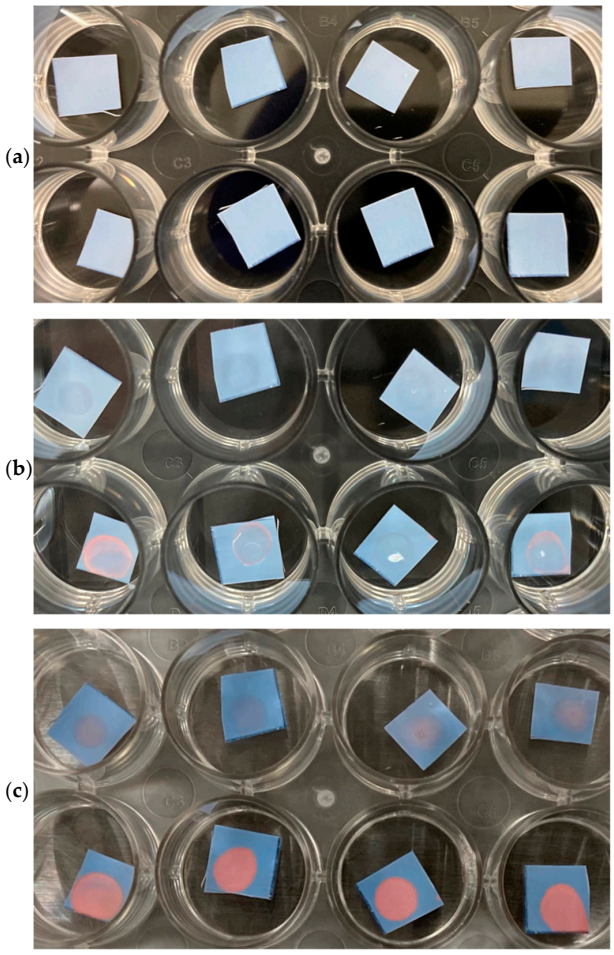


Figure 7. ACE2 substrates tested against SARS-CoV-2 Omicron-positive saliva (25 µL) (top row in quadruplicate), or against SARS-CoV-2 Delta-positive saliva (25 µL) (bottom row in quadruplicate). (**a**) Immediately after application, (**b**) after 2 h at RT, and (**c**) after 4 days at RT.

The PVDF-pDA-N-Antibody membranes were also tested against live and inactive COVID-19 saliva samples (Omicron). When the PVDF-pDA-N-Antibody membranes were exposed to a live virus, they did not initiate a color change, which was an expected response due to the entrapment of the N-protein within the viral particles (with RNA). However, the PVDF-pDA-N-Antibody membranes should have initiated a color change once exposed to the inactive, heated viral samples, as the N-protein would then be accessible, and a slight color change was observed (Figure 8). The heat process may have denatured the N-proteins just enough to prevent the antibody from recognizing them. An alternative and milder denaturing method will be used in future experiments, which will release the N-protein without destroying it.

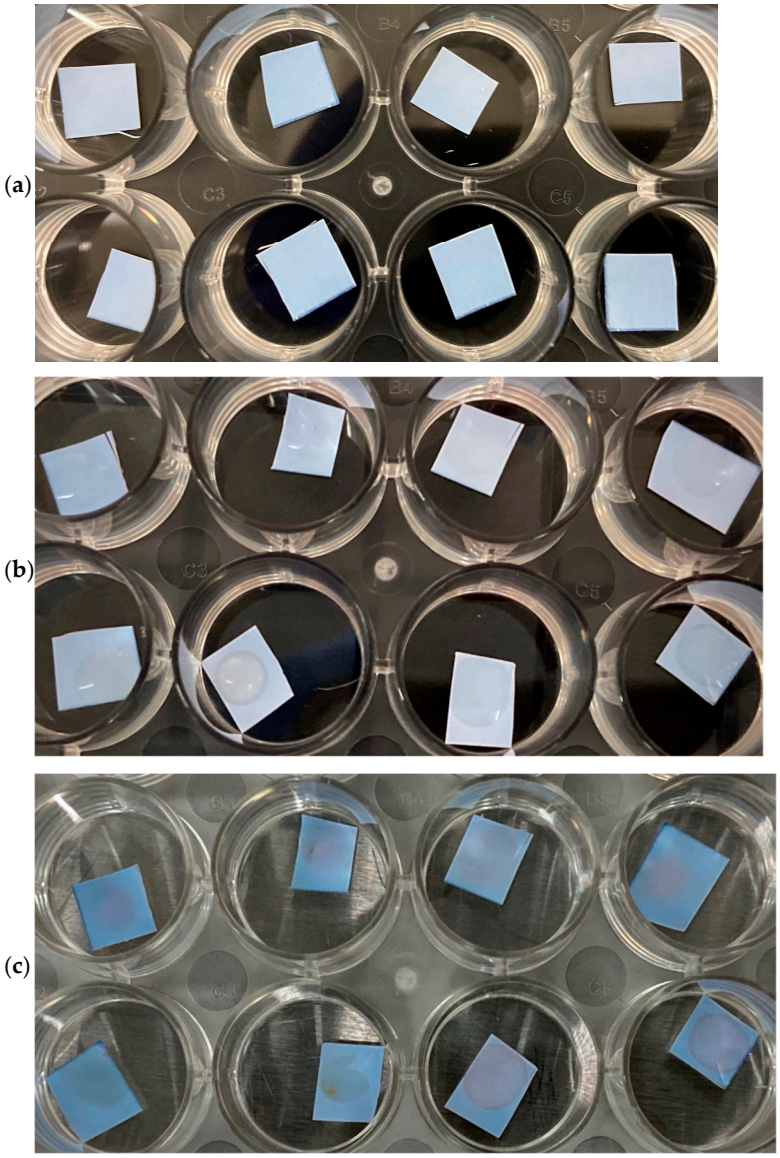


Figure 8. N-protein substrates tested against SARS-CoV-2 Omicron-positive saliva (25 µL) (top row in quadruplicate), or against SARS-CoV-2 Delta-positive saliva (25 µL) (bottom row in quadruplicate). (**a**) Immediately after application, (**b**) after 2 h at RT, and (**c**) after 4 days at RT.

3.6. Additional Testing of N-Antibody Protein Biosensor Membranes

The PVDF-pDA-N-Antibody membranes tested against live virus were unresponsive and did not initiate a color change once exposed to the saliva samples, as expected, due to the inability to access the N-protein entrapped within the viral particles. However, the PVDF-pDA-N-Antibody membranes should have initiated a color change once exposed

to the inactive viral samples, as the N-protein would be accessible, yet only slight color changes were observed. A possible reason why the N-protein membrane sensors did not initiate color changes once exposed to the virus was that additional components of the saliva samples inhibited the conjugated antibodies from recognizing the desired targets (i.e., N-proteins). To evaluate this possibility, the PVDF-pDA-N-Antibody membranes were tested against N-protein alone, N-protein plus a surfactant, N-protein plus COVID-19-negative saliva, an N-protein saliva mix, and controls. The PVDF-pDA-N-Antibody membranes were responsive to the N-protein, as we witnessed the desired color change in all the samples tested against the protein, whereas little to no color changes were observed in the controls tested against only a surfactant or saliva (Figure 9).

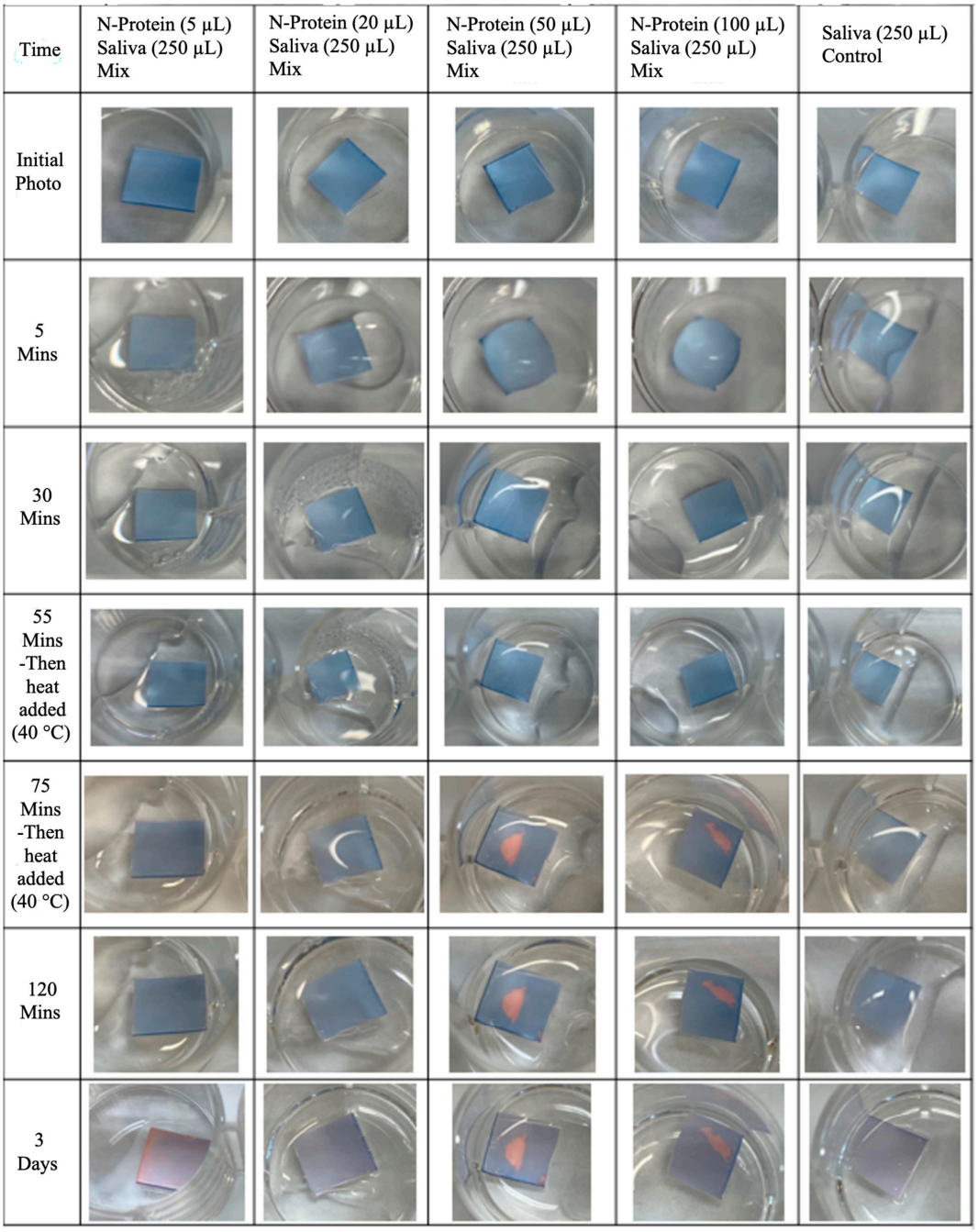


Figure 9. PVDF-pDA-N-Antibody membranes tested against saliva with different levels of N-protein added.

4. Conclusions

Eight different fabrics (nylon, polyester, acrylic, cotton) or membranes (PVDF, polypropylene, hydrophobic paper, filter paper) were tested for pDA surface-mounting, and PVDF was found to be the most suitable substrate for attaching pDAs. The PVDF-pDAs platforms had greater surface contact with the trigger protein, more dynamic color changes, and greater durability compared to the other substrates evaluated.

As shown in the SARS-CoV-2 human saliva testing against our sensing platforms, the ACE2/spike protein combination was more consistent than the nucleocapsid antibody/nucleocapsid protein combination in triggering the pDA color response. Eventually, multiple probes could be used for the sensor to minimize false negative responses and increase selectivity/positive responses.

Antibody and protein preparations used by suppliers differ; thus, the pH levels and buffers used in these protein preparations vary from one supplier to the next. These include phosphate buffers that can affect the sensor response. While these additives, such as phosphates, will not be present in native human samples, they do interfere with testing at this stage of sensor development, and they will be addressed as potentially interfering with the pDA sensor reactions. To address the interference of supplier additives and differences in how the proteins are prepared, we obtained ELISA kits that have matching antibody/protein pairs, so the interaction of these components was not a factor in the pDA sensor response. The results of the present study demonstrate that PVDF-pDA sensor platforms can be used to detect various biological molecules associated with SARS-CoV-2; thus, they pave the way for multiple biosensors on the same platform for increased reliability and sensitivity. Furthermore, as new variants appear, updated spike antibodies could be rapidly incorporated into sensing platforms and, eventually, multiple probes could be utilized in conjunction with one another on the sensor to minimize false negative responses while increasing selectivity and positive response rates.

Author Contributions: Conceptualization, T.W.H., P.L.D., J.K.N. and W.T.P.; methodology, C.T.S., T.W.H., P.L.D. and J.K.N.; validation, C.T.S. and B.C.; formal analysis, C.T.S., T.W.H., P.L.D. and J.K.N.; investigation, C.T.S. and B.C.; resources, T.W.H. and P.L.D.; writing—original draft preparation, C.T.S.; writing—review and editing, C.T.S., T.W.H., W.T.P. and P.L.D.; supervision, T.W.H., P.L.D. and J.K.N.; project administration, T.W.H., P.L.D. and J.K.N.; funding acquisition, T.W.H. and P.L.D. All authors have read and agreed to the published version of the manuscript.

Funding: This research was supported by a Prisma Healthcare seed grant and an award from the Intelligence Advanced Research Projects Activity, Office of the Director of National Intelligence, grant number IARPA-BAA-20-01, IARPA # U-909. The authors thank Dr. Delphine Dean, Clemson University, for active COVID-19 virus saliva samples, and Dr. Richard Hodinka, University of Pennsylvania, for helpful discussions on antigen selection and manipulation of viral particles.

Data Availability Statement: The dataset is available on request from the corresponding authors.

Conflicts of Interest: The authors declare no conflicts of interest. The funders had no role in the design of this study; in the collection, analyses, or interpretation of data; in the writing of the manuscript; or in the decision to publish the results.

References

1. D'Cruz, R.J.; Currier, A.W.; Sampson, V.B. Laboratory Testing Methods for Novel Severe Acute Respiratory Syndrome-Coronavirus-2 (SARS-CoV-2). *Front. Cell Dev. Biol.* **2020**, *8*, 468. [CrossRef]
2. Jianga, L.; Luoa, J.; Dong, D.; Wang, C.; Jin, W.; Xia, Y.; Wang, H.; Ding, H.; Jiang, L.; He, H. Development and evaluation of a polydiacetylene based biosensor for the detection of H5 influenza virus. *J. Virol. Methods* **2015**, *219*, 38–45. [CrossRef]

3. Vengesai, A.; Midzi, H.; Kasambala, M.; Mutandadzi, H.; Mduluza-Jokonya, T.L.; Rusakaniko, S.; Mutapi, F.; Naicker, T.; Mduluza, T. A systematic and meta-analysis review on the diagnostic accuracy of antibodies in the serological diagnosis of COVID-19. *Syst. Rev.* **2021**, *10*, 155. [CrossRef]
4. National Institute of Health. National Institute of Biomedical Imaging and Bioengineering. Available online: https://www.nibib.nih.gov/programs/radx-tech-program/authorized-tests (accessed on 30 May 2025).
5. Corman, V.M.; Landt, O.; Kaiser, M.; Molenkamp, R.; Meijer, A.; Chu, D.K.; Bleicker, T.; Brünink, S.; Schneider, J.; Schmidt, M.L.; et al. Detection of 2019 Novel Coronavirus (2019-nCoV) by Real-Time RT-PCR. *Euro Surveill.* **2020**, *25*, 2000045. [CrossRef]
6. Tahamtan, A.; Ardebili, A. Real-Time RT-PCR in COVID-19 Detection: Issues Affecting the Results. *Expert. Rev. Mol. Diagn.* **2020**, *20*, 453–454. [CrossRef] [PubMed]
7. Li, F. Structure, Function, and Evolution of Coronavirus Spike Proteins. *Annu. Rev. Viro.* **2016**, *3*, 237–261. [CrossRef]
8. Coutard, B.; Valle, C.; de Lamballerie, X.; Canard, B.; Seidah, N.G.; Decroly, E. The Spike Glycoprotein of the New Coronavirus 2019-nCoV Contains a Furin-like Cleavage Site Absent in CoV of the Same Clade. *Antivir. Res.* **2020**, *176*, 104742.
9. Hoffmann, M.; Kleine-Weber, H.; Schroeder, S.; Krüger, N.; Herrler, T.; Erichsen, S.; Schiergens, T.S.; Herrler, G.; Wu, N.-H.; Nitsche, A.; et al. SARS-CoV-2 Cell Entry Depends on ACE2 and TMPRSS2 and Is Blocked by a Clinically Proven Protease Inhibitor. *Cell* **2020**, *181*, 271–280. [CrossRef]
10. McBride, R.; van Zyl, M.; Fielding, B.C. The Coronavirus Nucleocapsid Is a Multifunctional Protein. *Viruses* **2014**, *6*, 2991–3018. [CrossRef] [PubMed]
11. Lu, X.; Pan, J.; Tao, J.; Guo, D. SARS-CoV Nucleocapsid Protein Antagonizes IFN-β Response by Targeting Initial Step of IFN-β Induction Pathway, and Its C-Terminal Region Is Critical for the Antagonism. *Virus Genes* **2010**, *42*, 37–45. [CrossRef] [PubMed]
12. Roy, V.; Fischinger, S.; Atyeo, C.; Slein, M.; Loos, C.; Balas, A.; Luedemann, C.; Astudillo, M.; Yang, D.; Wesemann, D.; et al. SARS-CoV-2-secific ELISA development. *J. Immunol. Methods* **2020**, *484–485*, 112832. [CrossRef]
13. Wu, L.; Li, G.; Xu, X.; Zhu, L.; Huang, R.; Chen, X. Application of nano-ELISA in foodanalysis: Recent advnaces and challenges. *Trends Anal. Chem.* **2019**, *113*, 140–156. [CrossRef]
14. Zhao, J.; Yuan, Q.; Wang, H.; Liu, W.; Liao, X.; Su, Y.; Wang, X.; Yuan, J.; Li, T.; Li, J.; et al. Antibody Responses to SARS-CoV-2 in Patients with Novel Coronavirus Disease. *Clin. Infect. Dis.* **2019**, *71*, 2027–2034. [CrossRef]
15. Okba, N.M.; Müller, M.A.; Li, W.; Wang, C.; GeurtsvanKessel, C.H.; Corman, V.M.; Lamers, M.M.; Sikkema, R.S.; de Bruin, E.; Chandler, F.D.; et al. SARS-CoV-2 specific antibody responses in COVID-19 patients. *MedRxiv* **2020**. [CrossRef]
16. Rai, P.; Kumar, B.K.; Deekshit, V.K.; Karunasagar, I.; Kaunasagar, I. Detection technologies and recent developments in the diagnosis of COVID-19 infection. *Appl. Microbiol. Biotechnol.* **2021**, *105*, 441–455. [CrossRef] [PubMed]
17. Wegner, G. Topochemische Reaktionen von Monomeren mit konjugierten Dreifachbindungen/Topochemical Reactions of Monomers with Conjugated Triple Bonds. *Z. Fur Naturforschung Sect. B-A J. Chem. Sci.* **1969**, *24*, 824–832. [CrossRef]
18. Charych, D.; Cheng, Q.; Reichert, A.; Kuziemko, G.; Stroh, M.; Nagyl, J.O.; Spevak, W.; Steven, R.C. A 'litmus test' for molecular recognition using artificial membranes. *Chem. Biol.* **1996**, *3*, 113–120. [CrossRef] [PubMed]
19. Lebègue, E.; Farre, C.; Jose, C.; Saulnier, J.; Lagarde, F.; Chevalier, Y.; Chaix, C.; Jaffrezic-Renault, N. Responsive Polydiacetylene Vesicles for Biosensing Microorganisms. *Sensors* **2018**, *18*, 599–615. [CrossRef]
20. Patra, S.; Shand, H.; Ghosal, S.; Ghorai, S. Harnessing polydiacetylene (PDA): A review of structural mechanics and infectious disease detection. *Next Mater.* **2025**, *8*, 100687. [CrossRef]
21. Jeong, H.-P.; Cho, E.; Yun, D.; Kim, T.; Lee, I.-S.; Jung, S. Label-Free Colorimetric Detection of Influenza Antigen Based on an Antibody-Polydiacetylene Conjugate and Its Coated Polyvinylidene Difluoride Membrane. *Polymers* **2017**, *9*, 127. [CrossRef]
22. Kharade, J.; Rodriguez, I.; Sanchez, V.; Materon, L.; Lozaono, K. Effect of Antimicrobial Metal Oxides on Molecular Arrangement and Sensing Ability of Polydiacetylene/Polyvinylidene Fluoride Nanofibers. *J. Appl. Polym. Sci.* **2025**, *142*, e57696. [CrossRef]
23. Park, H.K.; Chung, S.J.; Park, H.G.; Cho, J.-H.; Kim, M.; Chung, B.H. Mixed self-assembly of polydiacetylenes for highly specific and sensitive strip biosensors. *Biosens. Bioelectron.* **2008**, *24*, 480–484. [CrossRef]
24. Wen, J.T.; Viravathana, P.; Ingel, B.; Roper, C.; Tsutsui, H. Polydiacetylene-Coated Sensor Strip for Immunochromatic Detection of *Xylella fastidiosa* subsp. *fastidiosa*. *SLAS Tech.* **2017**, *22*, 406–412. [CrossRef]
25. Zhang, M.; Zhang, Q.; Ye, L. Colorimetric aptasensing of microcystin-LR using DNA-conjugated polydiacetylene. *Anal. Bioanal. Chem.* **2024**, *416*, 7131–7140. [CrossRef] [PubMed]
26. De Oliveira, T.V.; Soares, N.F.F.; Silva, D.J.; de Andrade, N.J.; Medeiros, E.A.A.; Badaró, A.T. Development of PDA/Phospholipids/Lysine Vesicles to Detect Pathogenic Bacteria. *Sens. Actuat. B Chem.* **2013**, *188*, 385–392. [CrossRef]
27. Bhattacharjee, A.; Goodall, E.; Popat, K.C.; Zou, L.; Li, Y.V. Selective detection of Gram-negative bacteria and antibacterial properties of colorimetric polydiacetylene nanofibers. *J. Mater. Sci.* **2023**, *58*, 8261–8273. [CrossRef]
28. Lehot, V.; Neuberg, P.; Ripoll, M.; Daubeuf, F.; Erb, S.; Dovgan, I.; Ursuegui, S.; Cianférani, S.; Kichler, A.; Chaubet, G.; et al. Targeted Anticancer Agent with Original Mode of Action Prepared by Supramolecular Assembly of Antibody Oligonucleotide Conjugates and Cationic Nanoparticles. *Pharmaceutics* **2023**, *15*, 1643. [CrossRef]

29. Son, S.U.; Seo, S.B.; Jang, S.; Choi, J.; Lim, J.-W.; Lee, D.K.; Kim, H.; Seo, S.; Kang, T.; Jung, J.; et al. Naked-Eye Detection of Pandemic Influenza a (pH1N1) Virus by Polydiacetylene (PDA)-Based Paper Sensor as a Point-of-Care Diagnostic Platform. *Sens. Actuat. B Chem.* **2019**, *291*, 257–265. [CrossRef]
30. Prainito, C.D.; Eshun, G.; Osonga, F.J.; Isika, D.; Centeno, C.; Sadik, O.A. Colorimetric Detection of the SARS-CoV-2 Virus (COVID-19) in Artificial Saliva Using Polydiacetylene Paper Strips. *Biosensors* **2022**, *12*, 804. [CrossRef]
31. Bhattacharjee, A.; Sabino, R.; Gangwish, J.; Manivasagam, V.; James, S.; Popat, K.; Reynolds, M.; Li, Y.V. A novel colorimetric biosensor for detecting SARS-CoV-2 by utilizing the interaction between nucleocapsid antibody and spike proteins. *Vitr. Models* **2022**, *1*, 241–247. [CrossRef]
32. Charych, D.H.; Nagy, J.O.; Spevak, W.; Bednarski, M.D. Direct Colorimetric Detection of a Receptor-Ligand Interaction by a Polymerized Bilayer Assembly. *Science* **1993**, *261*, 585–588. [CrossRef]
33. Kim, J.-M.; Ji, E.-K.; Woo, S.M.; Lee, H.; Ahn, D.J. Immobilized polydiacetylene vesicles on solid substrates for use as chemosensors. *Adv. Mater.* **2003**, *15*, 1118–1121. [CrossRef]
34. Peng, H.; Tang, J.; Yang, L.; Pang, J.; Ashbaugh, H.S.; Brinker, C.J.; Yang, Z.; Lu, Y. Responsive periodic mesoporous polydiacetylene/silica nanocomposites. *J. Am. Chem. Soc.* **2006**, *128*, 5304–5305. [CrossRef] [PubMed]
35. Meir, D.; Silbert, L.; Volinsky, R.; Kolusheva, S.; Weiser, I.; Jelinek, R. Colorimetric/fluorescent bacterial sensing by agarose-embedded lipid/polydiacetylene films. *J. Appl. Microbiol.* **2008**, *104*, 787–795. [CrossRef] [PubMed]
36. Kauffman, J.S.; Ellerbrock, B.M.; Stevens, K.A.; Brown, P.J.; Pennington, W.T.; Hanks, T.W. Preparation, characterization, and sensing behavior of polydiacetylene liposomes embedded in alginate fibers. *ACS Appl. Mater. Interfaces* **2009**, *1*, 1287–1291. [CrossRef]
37. Wang, X.; Sun, X.; Hu, P.A.; Zhang, J.; Wang, L.; Feng, W.; Lei, S.; Yang, B.; Cao, W. Colorimetric Sensor Based on Self- Assembled Polydiacetylene/Graphene-Stacked Composite Film for Vapor-Phase Volatile Organic Compounds. *Adv. Funct. Mater.* **2013**, *23*, 6044–6050. [CrossRef]
38. Jung, S.-H.; Jang, H.; Lim, M.-C.; Kim, J.-H.; Shin, K.-S.; Kim, S.M.; Kim, H.-Y.; Kim, Y.-R.; Jeon, T.-J. Chromatic Biosensor for Detection of Phosphinothricin Acetyltransferase (PAT) using Polydiacetylene Vesicles Encapsulated Within Automatically Generated Immuno-Hydrogel Beads. *Anal. Chem.* **2015**, *87*, 2072. [CrossRef]
39. Zhang, Y.; Dawson, P.L.; Hanks, T.W.; Northcutt, J.K.; Tzeng, T.-R.; Pennington, W.T. Detecting and Correlating Bacterial Populations to Visual Color Change of Polydiacetylene-Coated Filters. *Talanta* **2020**, *221*, 121482. [CrossRef]
40. Wen, J.T.; Bohorquez, K.; Tsutsui, H. Polydiacetylene-Coated Polyvinylidene Fluoride Strip Aptasensor for Colorimetric Detection of Zinc (II). *Sens. Actuat.* **2016**, *232*, 313–317. [CrossRef]
41. Yoon, B.; Lee, S.; Kim, J.-M. Recent conceptual and technological advances in polydiacetylene-based supramolecular chemosensors. *Chem. Soc. Rev.* **2009**, *38*, 1958–1968. [CrossRef]
42. Zhang, Y.; Northcutt, J.; Hanks, T.W.; Miller, I.; Pennington, W.T.; Jelinek, R.; Han, I.; Dawson, P. Polydiacetylene sensor interaction with food sanitizers and surfactants. *Food Chem.* **2017**, *221*, 515–520. [CrossRef]
43. Zhou, Y.; Xue, Y.; Lin, X.; Duan, M.; Hong, W.; Geng, L.; Zhou, J.; Fan, Y. Smartphone-based polydiacetylene colorimetric sensor for point-of-care diagnosis of bacterial infections. *Smart Mater. Med.* **2024**, *5*, 140–162. [CrossRef]
44. Fang, X.; Ye, L.B.; Zhang, Y.; Li, B.; Li, S.; Kong, L.; Wang, Y.; Zheng, H.; Wang, W.; Wu, Z. Nucleocapsid amino acids 211 to 254, in particular, tetrad glutamines, are essential for the interaction between the nucleocapsid and membrane proteins of SARS-associated coronavirus. *J. Microbiol.* **2006**, *44*, 577–580. [PubMed]
45. Luo, H.; Chen, Q.; Chen, J.; Chen, K.; Shen, X.; Jiang, H. The nucleocapsid protein of SARS coronavirus has a high binding affinity to the human cellular heterogeneous nuclear ribonucleoprotein A1. *FEBS Lett.* **2005**, *579*, 2623–2628. [CrossRef] [PubMed]

Disclaimer/Publisher's Note: The statements, opinions and data contained in all publications are solely those of the individual author(s) and contributor(s) and not of MDPI and/or the editor(s). MDPI and/or the editor(s) disclaim responsibility for any injury to people or property resulting from any ideas, methods, instructions or products referred to in the content.